Am J Cancer Res 2017;7(5):1177-1187
www.ajcr.us /ISSN:2156-6976/ajcr0052124

Original Article

MicroRNA-338-3p inhibits thyroid cancer progression through targeting AKT3

Guo-Qing Sui, Dan Fei, Feng Guo, Xi Zhen, Qiang Luo, Shuai Yin, Hui Wang

Department of Ultrasound, The China-Japan Union Hospital of Jilin University, Changchun 130033, China

Received March 3, 2017; Accepted March 15, 2017; Epub May 1, 2017; Published May 15, 2017

Abstract: microRNA-338-3p (miR-338-3p) has been implicated in tumor development and progression in many types of cancers. However, the function and mechanism underlying the action of miR-383-3p in thyroid cancer remain unclear and were therefore investigated in this study by *in vitro* and *in vivo* experiments. We found that miR-338-3p was downregulated in thyroid cancer tissues and cell lines. miR-338-3p expression was significantly associated with the clinical stage and lymph node metastasis of thyroid cancer. Forced expression of miR-338-3p suppressed thyroid cancer cell proliferation, clonogenicity, migration, and invasion *in vitro* and inhibited tumorigenesis in a nude mouse xenograft model system. Moreover, AKT3, a known oncogene, was confirmed as a direct target of miR-383-3p in thyroid cancer cells, as evidenced by the fact that ectopic miR-383 expression suppressed AKT3 expression and its downstream pathway (AKT pathway). In addition, AKT3 silencing by siRNA mimicked the effect of ectopic miR-338-3p on the growth and invasion of thyroid cancer cells. In contrast, AKT3 overexpression attenuated the inhibitory effect induced by miR-338-3p overexpression in thyroid cancer cells. These results suggest that miR-338-3p functions as a novel tumor suppressor that blocks thyroid cancer cell growth through targeting *AKT3.*

Keywords: Thyroid cancer, miR-338-3p, AKT3, proliferation, invasion

Introduction

Thyroid cancer is the most prevalent endocrine neoplasm; its prevalence has been rapidly increasing in many countries over the last several decades [1]. Although the prognosis of most patients with thyroid cancer is extremely good, a significant proportion of patients exhibit locoregional recurrence or distant metastases within 10 years [2, 3]. Therefore, it is extremely important to elucidate the molecular mechanisms underlying carcinogenesis and progression in thyroid cancer, which would contribute to providing promising therapeutic targets for thyroid cancer and improving the prognosis of this disease.

microRNAs (miRNAs) are a class of small (18-25 nucleotides in length), endogenously expressed, well-conserved noncoding RNA molecules that regulate gene expression at the post-transcriptional level by binding to the 3'-untranslated region (UTR) of target mRNAs [4]. miRNAs have been reported to be involved in diverse biological processes, such as cell growth, migration, invasion, apoptosis, metabolism, and cellular differentiation [5]. Given that more than 50% of miRNAs are located in cancer-associated genomic regions or in fragile sites, miRNAs have been recognized as key regulators in cancer development and progression [6, 7]. Various studies have indicated that alterations in miRNA expression are involved in the initiation, development, and progression of thyroid cancer, and could act as a diagnostic marker or therapeutic agent for thyroid cancer [8-10].

miR-338-3p, located on the seventh intron of the apoptosis-associated tyrosine kinase (AATK) gene, has been reported to be downregulated and to function as a tumor suppressor in many types of cancers, such as non-small cell lung cancer [11], ovarian cancer [12], hepatocellular carcinoma [13], glioma [14], and gastric cancer [15, 16]. However, the clinicopathological impact and the biological function of miR-338-3p in thyroid cancer and the underlying molecular mechanisms remain unclear.

In the current study, we first investigated the clinicopathological effect of miR-338-3p on patients with thyroid cancer and found that miR-338-3p expression in thyroid cancer tissues was significantly lower than that in the adjacent noncancerous tissues (ANTs) and that its expression was negatively related with the clinical stage and lymph node metastasis. We also investigated the role of miR-338-3p in thyroid cancer, both in *vitro* and *in vivo*, and found that miR-338-3p overexpression significantly suppressed thyroid cancer cell proliferation, migration, and invasion in *vitro* and inhibited tumor growth in *vivo* through targeting *AKT3* Overall, considering the strong suppressive effect of miR-338-3p on thyroid cancer, it can be considered as a potential therapeutic target for this disease.

Materials and methods

Patients and tissue samples

Thyroid cancer tissues and the corresponding adjacent noncancerous tissues (ANTs) were obtained from 48 patients who had thyroid cancer and had undergone surgery at the China-Japan Union Hospital of Jilin University (Changchun, China) between July 2014 and July 2016. Noncancerous tissues adjacent to the tumor were obtained from 3 cm away from the tumor cells, and the lack of tumor cell infiltration was verified by pathological examination. All tissue samples were immediately frozen in liquid nitrogen and stored at -80°C until RNA extraction. All patients had not received chemotherapy or radiotherapy before surgery. Informed consent was obtained from each patient and the study protocol and consent procedures were approved by the ethics committee of China-Japan Union Hospital of Jilin University (Changchun, China).

Cell lines and culture

The human thyroid cancer cell lines 8505C, TPC-1, and SW1736 and the human thyroid follicular epithelial cell line Nthy-ori3-1 were obtained from the Type Culture Collection of the Chinese Academy of Sciences (Shanghai, China). They were cultured in RPMI1640 medium (Gibco, USA) supplemented with 10% fetal bovine serum (FBS; Gibco), penicillin (100 units/ml, Sigma Aldrich, St. Louis, MO, USA), or streptomycin (100 μg/ml; Sigma Aldrich). The cells were maintained at 37°C in a humidified chamber supplemented with 5% CO_2.

Transient transfection

The miR-338-3p mimic (miR-338-3p) and corresponding negative control mimic (miR-NC) were purchased from GenePharma (Shanghai, China), and siRNA against AKT3 (si-AKT3), siRNA against negative control (si-NC), and the AKT3-overexpressing plasmid were provided by Dr. Rui Li (Jilin University, Changchun, China). These molecular products were transfected into thyroid cancer cells by using Lipofectamine 2000 (Invitrogen, Carlsbad, CA, USA) for various experiments according to manufacturer's instructions. Each experiment was repeated three times each in triplicates.

RNA extraction and quantitative real time PCR (qRT-PCR)

miRNA extraction was performed with the mirVana miRNA Isolation Kit (Ambion, USA) from tumor tissue sections or cultured cells. miR-338-3p expression was determined using the SYBR Primescript miRNA RT-qPCR kit (Toyobo, Osaka, Japan), and primers for miR-338-3p or U6 (Applied Biosystems, Foster City, CA, USA) with the ABI 7900 Sequence Detection System (Applied Biosystems). U6 was used as an endogenous control for miRNAs.

Total RNA of cells and tissues was extracted using TRIzol (Invitrogen) and was reverse transcribed to cDNA using the Primer Script RT reagent Kit (TaKaRa Bio, Japan). cDNA was then analyzed using the Fast SYBR Green Master Mix (Applied Biosystems) with the ABI 7900 Sequence Detection System. The housekeeping gene glyceraldehyde phosphate dehydrogenase (GAPDH) was used as an internal control for mRNAs. The AKT3 and GAPDH primers used in this study have been described previously [17]. The relative expression of miR-338-3p and AKT3 was analyzed by the $2^{-\Delta\Delta Ct}$ method.

Cell proliferation and colony formation assays

In vitro cell proliferation was measured using the 3-(4,5-dimethylthiazol-2-yl)-2,5-diphenyltetrazolium bromide (MTT) method following the protocol reported in our previous study [18].

For the colony formation assay, transfected cells were seeded into 6-well plates at a density of 300 cells per well. After culture for 14 days, the colonies were washed twice with PBS, fixed with 4% paraformaldehyde, and stained with 1% crystal violet. The colonies were imaged and counted in five randomly selected fields under a light microscope (Olympus, Tokyo, Japan).

Cell migration and invasion assays

Cell migration was determined using a wound healing assay. Briefly, cells (5.0×10^4) were seeded in 6-well plates and incubated for 24 h after transfection. A wound was created with a pipette tip, and a photograph was obtained under a light microscope (Olympus). After incubation for 24 h, photographs were again obtained at the same position under a light microscope. The wound gaps were measured per time point.

Cell invasiveness was assessed with a Transwell chamber (Corning, Tewksbury, Massachusetts, USA) in which the two chambers were separated by a Matrigel-coated polycarbonate membrane (pore size, 8 μm). Briefly, 1×10^5 transfected cells were placed into the upper chambers precoated with Matrigel (BD, Franklin Lakes, NJ, USA) in serum-free medium. The lower chambers were filled with 600 μl of complete medium containing 10% FBS as chemoattractant. After the cells had been cultured at 37°C for 48 h, the cells on the upper membrane surface were removed, whereas the invasive cells that attached to the lower surface of the membrane insert were fixed with 70% ethanol for 30 min and stained with 0.1% crystal violet for 10 min. Then, cells were counted in five randomly selected fields per well under a light microscope (Olympus).

Luciferase reporter assay

The wild-type (WT) or mutant-type (MUT) seed region at the 3'UTR of AKT3 was synthesized and cloned into the downstream region of a firefly luciferase cassette in the pGL3-promoter vector (Promega, Madison, WI, USA) as per the manufacturer's instructions. The TPC-1 cells were cotransfected with vectors carrying the WT 3'UTR or MUT 3'UTR AKT3 and miR-338-3p mimic or miR-NC by using Lipofectamine2000 reagent according to the manufacturer's instructions. After 48 h of transfection, the cells were harvested to detect luciferase activity by using the Dual-Luciferase Assay (Promega) as per the manufacturer's instructions.

Western blot

Total proteins were extracted from cells or tissues with RIPA buffer (10 mM Tris-HCl, pH 7.4, 1% Triton X-100, 0.1% SDS, 1% NP-40, 1 mM $MgCl_2$) containing protease inhibitors. The total protein concentration was determined using a BCA Protein Assay Kit (Vigorous Biotechnology Beijing Co. Ltd, Beijing, China). A total of 30 mg of protein was separated on a 10% SDS-polyacrylamide gel and then transferred onto polyvinylidene fluoride (PDVF) membranes (Sigma Aldrich). The membranes were blocked with 5% nonfat milk and then incubated with primary antibodies against AKT3, p-AKT, and GAPDH (all antibodies from Santa Cruz Biotechnology, CA, USA) overnight at 4°C. On the following day, the blots were washed with PBST and incubated with horseradishperoxidase-conjugated secondary antibodies (Santa Cruz) for 2 h at room temperature. The protein band was visualized by chemiluminescence with Pierce ECL kits (Millipore, MA, USA). GAPDH was used as an internal control.

Tumor xenograft treatment model

All experimental procedures involving animals were approved by the Ethics Committee of Jilin University (Changchun China). Male BALB/c mice (age, 4 weeks) were maintained under specificpathogen-free (SPF) conditions under a 12 h light/dark cycle. The mice were divided into two groups (n=10 each); they were inoculated with TPC-1 cells stably expressing miR-338-3p or miR-NC via subcutaneous injection of 2×10^6 cells (100 μl) into the left flank. Xenograft growth was measured every 5 days, beginning at day 10. Xenograft volume (V) was monitored by measuring the length (L) and width (W) with calipers and was calculated as $V = 0.5 \times L$ (length) $\times W^2$ (width). The mice were sacrificed 30 days after injection. The tumor tissues were dissected, weighted, and stored at -80°C until use.

Statistical analysis

Statistical analysis was performed using the SPSS software (version 16.0, Chicago, IL). Statistical analysis between two samples was

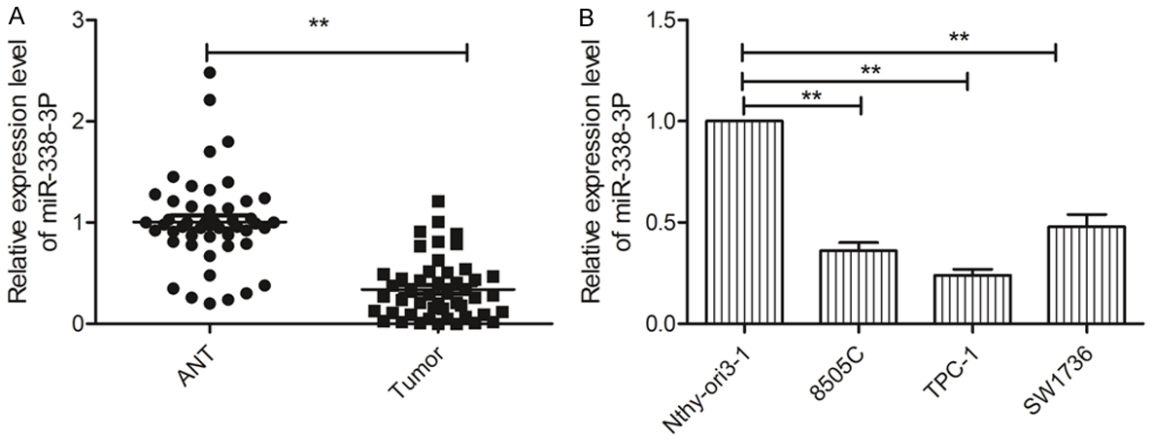

Figure 1. Aberrant expression of miR-338-3p was noted in thyroid cancer tissues and cell lines. A. miR-338-3p expression levels in 48 thyroid cancer tissues and adjacent noncancerous tissues (ANTs) were evaluated by qRT-PCR. B. miR-338-3p expression levels in three thyroid cancer cell lines (8505C, TPC-1, and SW1736) and in a human thyroid follicular epithelial cell line (Nthy-ori 3-1) were evaluated using qRT-PCR. *P < 0.05, **P < 0.01.

Table 1. Correlation between clinicopathological features and miR-338-3pexpression in thyroid cancer tissues

Variables	No. of cases	miR-338-3p expression		*P* value
		Low (n %)	High (n %)	
Age (years)				P > 0.05
< 60	22	12 (54.5)	10 (45.5)	
≥ 60	26	14 (53.8)	12 (46.2)	
Gender				P > 0.05
Male	19	10 (52.6)	9 (47.2)	
Female	29	16 (55.2)	13 (44.8)	
TNM stage				P < 0.01
T1-T2	34	16 (47.1)	18 (52.9)	
T3-T4	14	10 (71.4)	4 (28.6)	
Tumor size				P > 0.05
< 3	31	15 (48.4)	16 (51.2)	
≥ 3	17	11 (64.7)	6 (35.3)	
Lymph node metastasis				P < 0.01
No	35	14 (40.0)	21 (60.0)	
Yes	13	12 (92.3)	1 (7.7)	

performed using the Student t-test, and for more than two groups, using one-way ANOVA. Spearman correlation test was used for analyzing the correlations between the miR-338-3pand AKT3 expression levels. P < 0.05 was considered statistically significant.

Results

miR-338-3p expression was downregulated in thyroid cancer tissues and cell lines

Using qRT-PCR, miR-338-3p expression was detected in thyroid cancer tissues and their matched ANTs from 48 patients. miR-338-3p expression was lower in thyroid cancer samples than in ANTs (**Figure 1A**). To further investigate the clinical significance of miR-338-3p in thyroid cancer, the 48 patients were divided into two groups according to the median value (0.34) of miR-383-3p expression in thyroid cancer tissues: high-expression group (> 0.34, n=22) and low-expression group (< 0.34, n=26). Statistical analysis showed that the miR-383-3p expression level was significantly negatively related to lymph node metastasis and the clinical stage (**Table 1**), both of which are indicators of poor prognosis.

In addition, we evaluated miR-338-3 pexpression in three thyroid cancer cell lines (8505C, TPC-1, and SW1736) and a human thyroid follicular epithelial cell lines (Nthy-ori3-1). In all the thyroid cancer cell lines, miR-338-3p expression was lower than that in Nthy-ori 3-1 cells; the difference varied across cell lines (**Figure 1B**).

miR-338-3p inhibited thyroid cancer growth in vitro and in vivo

To assess the biological effects of miR-338-3p in thyroid cancer cells, a miR-338-3p mimic was transfected into TPC-1 cells, which had the lowest expression from the three cell lines

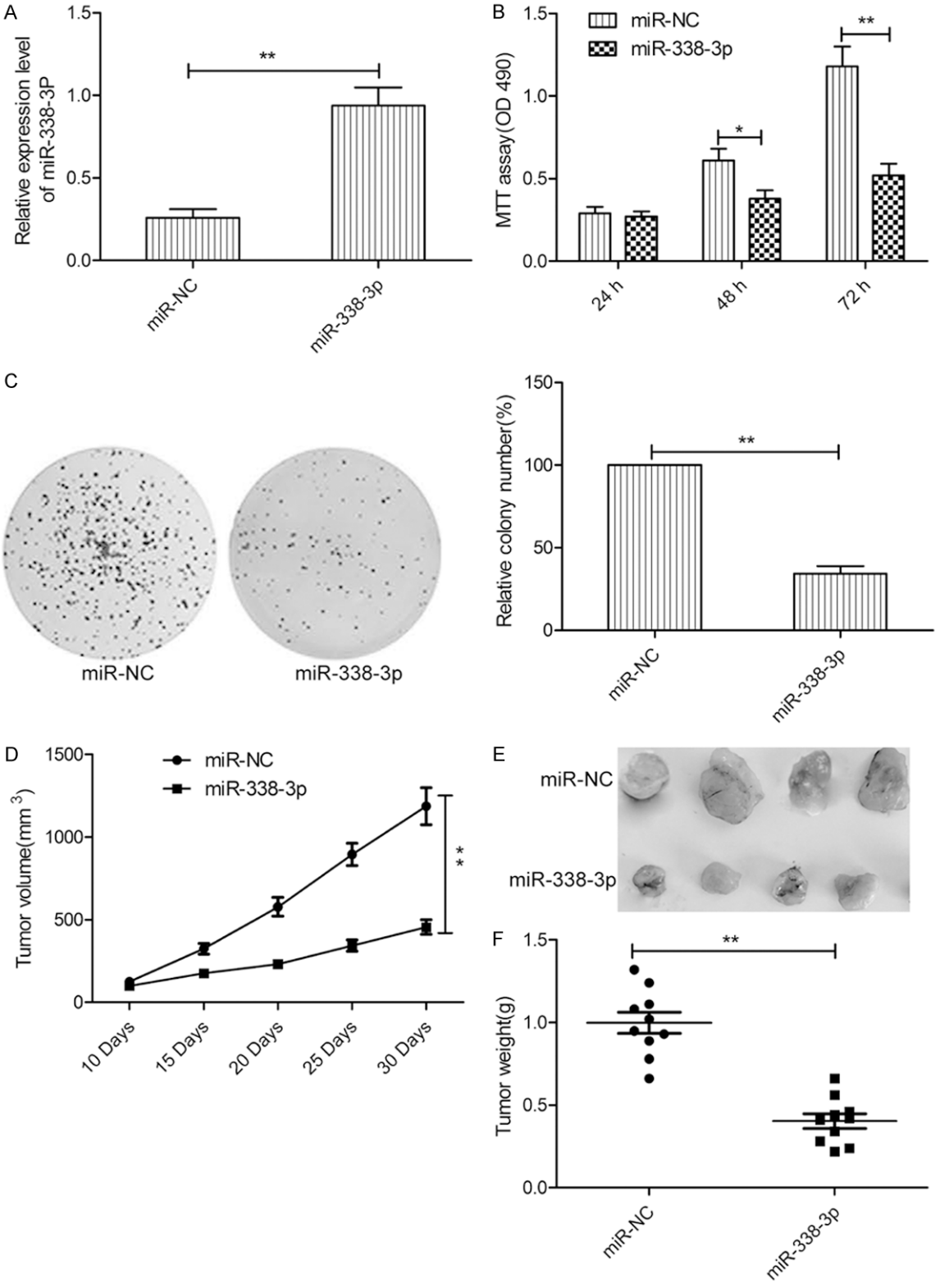

Figure 2. miR-338-3p inhibits thyroid cancer growth *in vitro* and *in vivo*. A. miR-338-3p expression levels were evaluated by qRT-PCR in TPC-1 cells after transfection with the miR-338-3p mimic or miR-NC. B, C. Cell proliferation and colony formation were determined in TPC-1 cells after transfection with the miR-338-3p mimic or miR-NC. D. Tumor growth curves for the miR-338-3p and miR-NC groups. E. Tumor images for the miR-338-3p and miR-NC groups. F. Tumor weights for the miR-338-3p and miR-NC groups. *P < 0.05, **P < 0.01.

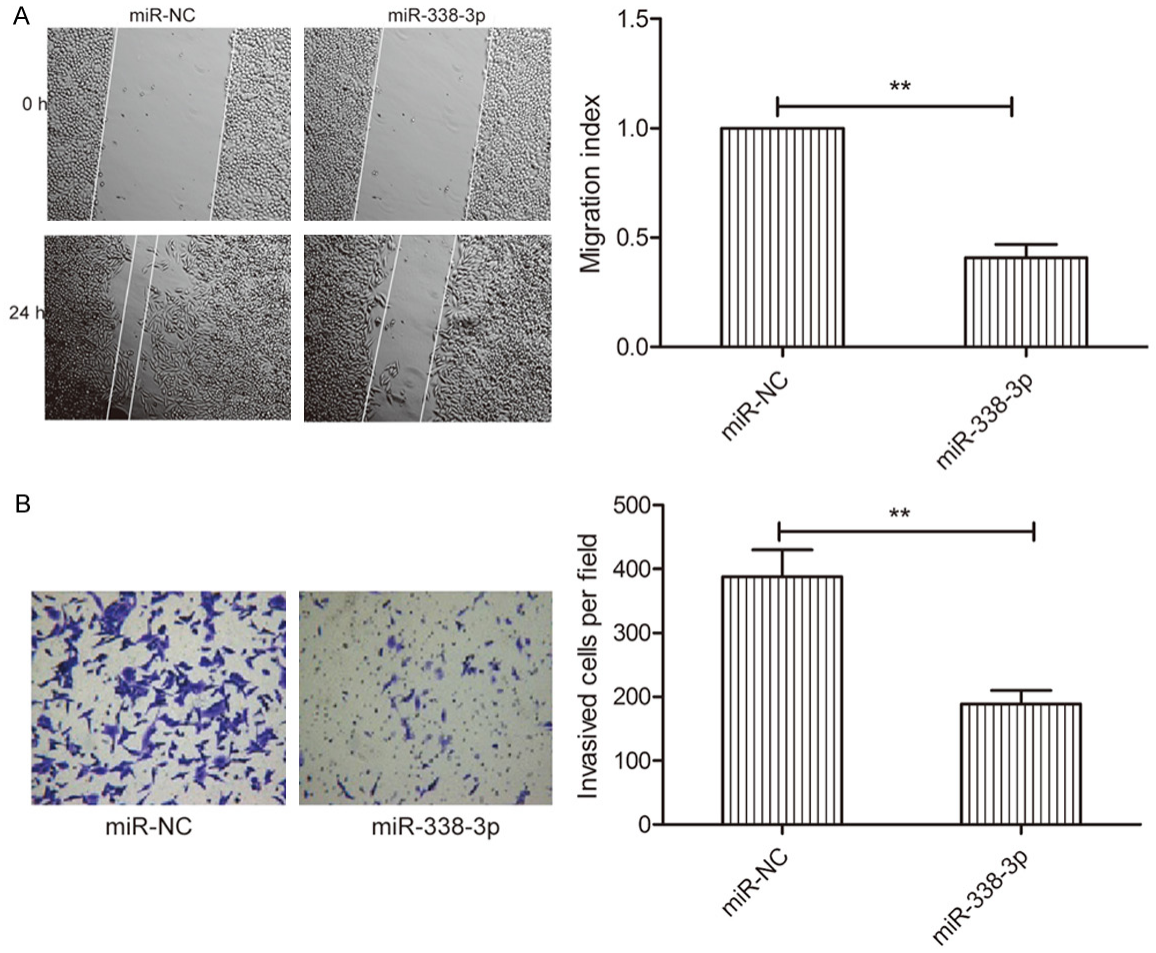

Figure 3. miR-338-3p inhibits thyroid cancer cell migration and invasion. A. Wound healing was performed to detect migration of TPC-1 cells transfected with miR-338-3p or miR-NC. B. Transwell invasion chamber was used to detect the invasion of TPC-1 cells transfected with miR-338-3p or miR-NC. *P < 0.05, **P < 0.01.

(**Figure 1B**). miR-338-3p transfection was successful and significantly increased the miR-338-3p expression level in TPC-1 cells (**Figure 2A**). The MTT assay results revealed that miR-338-3p overexpression in TPC-1 cells significantly reduced proliferation (**Figure 2B**). To further assess the effect of miR-338-3p on cell proliferation, a colony formation assay was used. miR-338-3p overexpression also significantly decreased colony formation of TPC-1 cells (**Figure 2C**). To confirm the above data *in vivo*, we created tumor xenograft mouse models. miR-338-3p overexpression significantly inhibited tumor growth *in vivo* (**Figure 2D**). The size of subcutaneous tumors and weight derived from miR-338-3p-expressing TPC-1 cells were dramatically lower than those of miR-NC-expressing cells (**Figure 2E** and **2F**).

miR-338-3p inhibited thyroid cancer cell migration and invasion

To study the effect of miR-338-3p on the metastasis ability of thyroid cancer cells, migration and invasion analyses were performed for TPC-1 cells transfected with miR-338-3p or miR-NC by wound healing and invasion chamber assays, respectively. miR-338-3p restoration significantly decreased migration (**Figure 3A**) and invasion (**Figure 3B**) capacity in TPC-1 cells.

AKT3 is a direct target of miR-338-3p

To understand the mechanisms by which miR-338-3p suppressed thyroid cancer growth, we searched for candidate targets of miR-338-3p that might play a role in thyroid cancer patho-

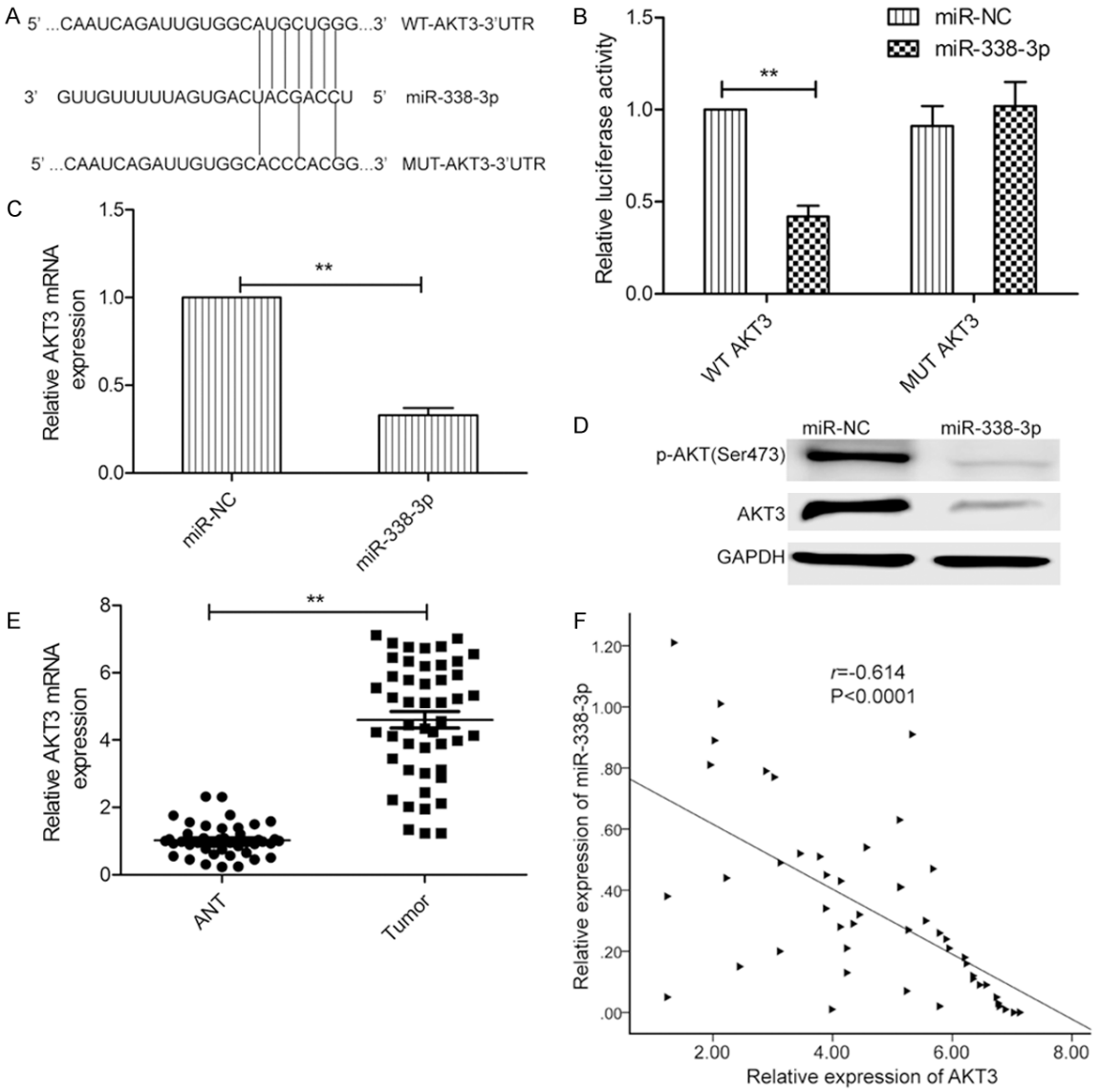

Figure 4. AKT3 is a direct target of miR-338-3p. A. The predicted binding sites for miR-338-3p in the 3'-UTR of AKT3 and the mutations in the binding sites are shown. B. Luciferase activity was determined in TPC-1 cells cotransfected with the miR-338-3p mimic or miR-NC and a luciferase reporter plasmid (WT/MUT 3'UTR AKT3). C. The AKT3 mRNA level was analyzed using qRT-PCR in TPC-1 cells transfected with the miR-338-3p mimic or miR-NC. GAPDH was used as an internal control. D. AKT3 and p-AKT proteins were analyzed in TPC-1 cells transfected with the miR-338-3p mimic or miR-NC by western blot. GAPDH was used as an internal control. E. AKT3 mRNA levels in 48 thyroid cancer tissues and ANTs were evaluated by qRT-PCR. GAPDH was used as an internal control. F. The inverse relationship between AKT3 and miR-338-3p expression was investigated in thyroid cancer tissue samples by Spearman's correlation assay (n=48).

genesis, using the miRanda, TargetScan, and PicTar algorithms. We identified the 3'-UTR of AKT3 that was able to bind to the seed region of miR-338-3p (**Figure 4A**). To further confirm the binding of miR-338-3p to the 3'-UTR of AKT3, we performed a luciferase assay. miR-338-3p was found to bind to the 3'-UTR, which resulted in a marked decrease in luciferase activities (**Figure 4B**). In addition, miR-338-3p overexpression significantly inhibited expression of AKT3 (**Figure 4C** and **4D**) and of its downstream protein, p-AKT, which caused AKT pathway inhibition (**Figure 4D**). Importantly, we found that the AKT3 mRNA level in thyroid cancer tissues was much higher than that in ANTs (**Figure 4E**), and that the AKT3 mRNA expres-

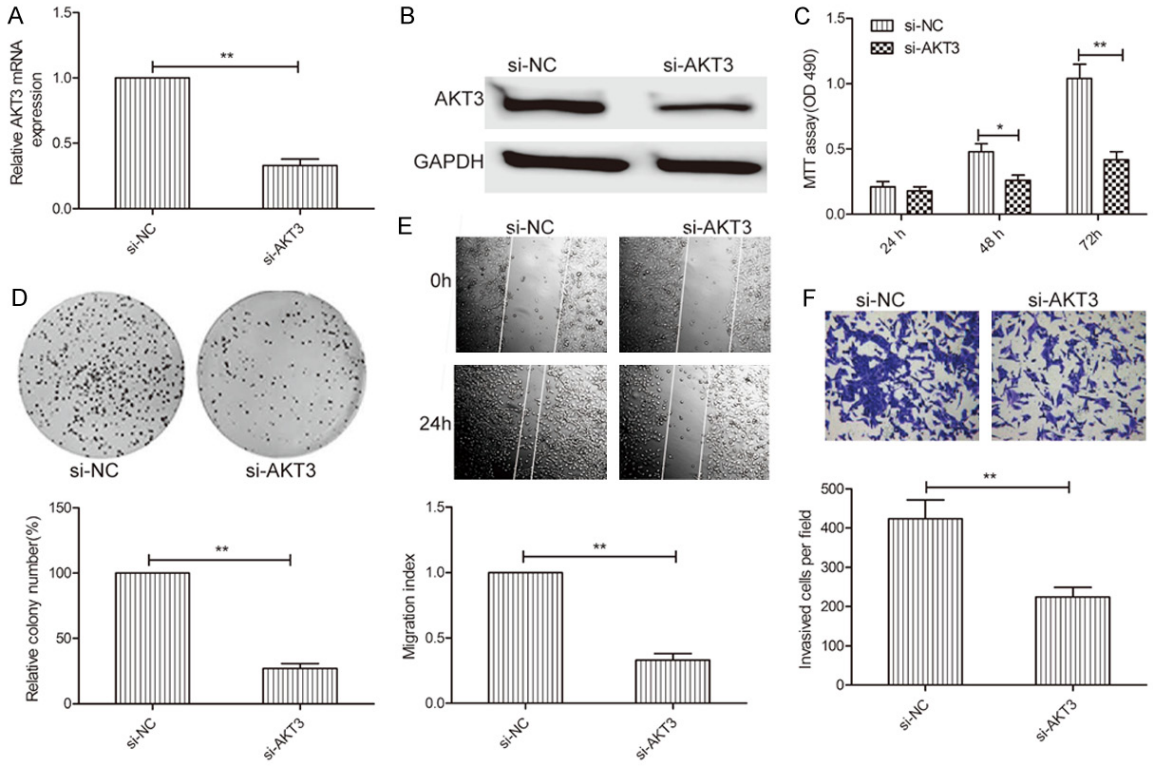

Figure 5. AKT3 downregulation mimicked the inhibitory effect of miR-338-3p overexpression in thyroid cancer cells. (A, B) AKT3 mRNA (A) and protein (B) levels were determined in TPC-1 cells transfected with si-AKT3 or si-NC. GAPDH was used as an internal control. (C-F) Cell proliferation, colony formation, migration, and invasion were analyzed in TPC-1 cells transfected with si-AKT3 or si-NC. *P < 0.05, **P < 0.01.

sion level was inversely correlated withmiR-338-3p expression in thyroid cancer tissues (**Figure 4F**; *r*=-0.614, P < 0.0001). These data suggest that AKT3 is a target of miR-338-3p in thyroid cancer.

Silencing of AKT3 and overexpression of miR-338-3p had similar effects in thyroid cancer cells

To investigate the biological functions of AKT3 in thyroid cancer cells, AKT3 expression was silenced in TPC-1 cells by transfection with si-AKT3 or si-NC. qRT-PCR and western blot assays confirmed that AKT3 expression in TPC-1 cells transfected with si-AKT3 was significantly lower than that in cells transfected with miR-NC (**Figure 5A** and **5B**). Functional assays showed that AKT3 downregulation significantly inhibited cell proliferation (**Figure 5C**) and colony formation (**Figure 5D**), migration (**Figure 5E**), and invasion (**Figure 5F**) in TPC-1 cells, which mimicked the inhibitory effect of miR-338-3p overexpression in TPC-1 cells.

AKT3 overexpression rescued the miR-338-3p-mediated inhibitory effect on thyroid cancer cells

To further determine whether *AKT3* is a functional target of miR-338-3p in thyroid cancer cells, we performed a rescue experiment involving transfection of AKT3 plasmids into miR-338-3p-expressing TPC-1 cells. TPC-1 transfected with the AKT3-overexpressing plasmid showed restoration of AKT3 expression, which caused reduction via miR-338-3p overexpression (**Figure 6A** and **6B**). In addition, AKT3 overexpression in TPC-1 cells could rescue the inhibitory effect of miR-338-3p on cell proliferation, colony formation, migration, and invasion (**Figure 6C-F**). Taken together, these results indicated that miR-338-3p exerted its suppressive effects in thyroid cancer by repressing *AKT3*.

Discussion

A series of studies reported that altered expression of miRNAs is involved in the initiation and

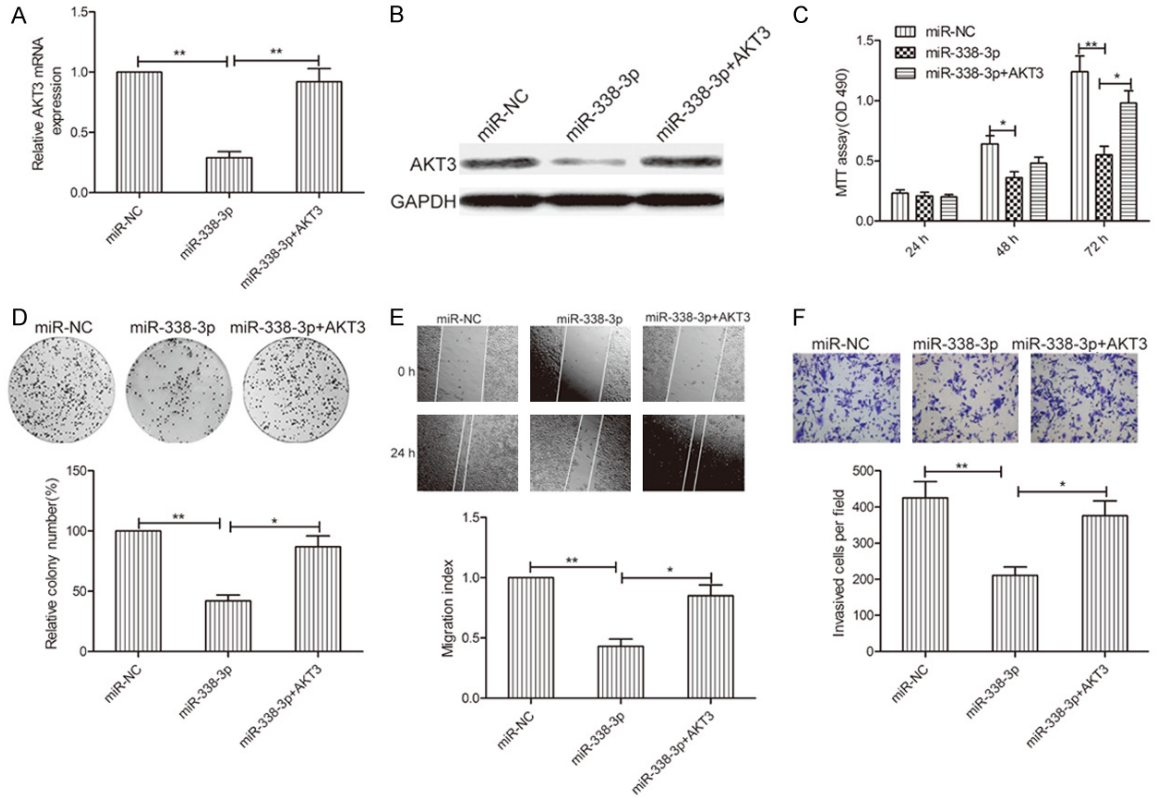

Figure 6. AKT3 overexpression rescues the miR-338-3p-mediated inhibitory effect on thyroid cancer cells. (A, B) AKT3 mRNA (A) and protein (B) expression levels were analyzed in TPC-1 cells transfected with miR-338-3p or miR-NC, with/without the AKT3-overexpressing plasmid. (C-F) Cell proliferation, colony formation, migration, and invasion were analyzed in TPC-1 cells transfected with miR-338-3p or miR-NC, with/without the AKT3-overexpressing plasmid. *P < 0.05, **P < 0.01.

progression of thyroid cancer [8-10]. For example, Wang *et al* reported that miR-497 inhibits thyroid cancer cell proliferation, colony formation, migration, and invasion by repressing BDNF and its downstream signaling pathways (PI3K/AKT) [19]. Wen *et al* found that miR-126 restoration in thyroid cancer cells markedly inhibited cell proliferation, migration, and invasion by repressing LRP6 [18]. Dong *et al* demonstrated that miR-141 overexpression inhibited cell proliferation, induced cell apoptosis, decreased migration and invasion in thyroid cancer cells, and retarded tumor growth in nude mice by targeting insulin receptor substrate 2 (IRS2) [20]. In the current study, we found that miR-338-3p was downregulated in both thyroid cancer tissues and thyroid cancer cell lines and that miR-338-3p overexpression significantly inhibited cell proliferation, colony formation, migration, and invasion, as well as suppressed *in vivo* tumor formation by targeting *AKT3*. These results suggest that miR-338-3p is a potential therapeutic target for thyroid cancer.

Recent studies have shown that miR-338-3p expression is downregulated and that it functions as a tumor suppressor in various types of cancers [11-16, 21, 22]. However, the biological role of miR-338-3p in thyroid cancer remains unclear. In the current study, we found that miR-338-3p was frequently downregulated in both thyroid cancer tissues and thyroid cancer cell lines. Moreover, miR-338-3p expression was significantly correlated with clinical stage and lymph node metastasis. Given that miR-338-3p was downregulated in thyroid cancer tissues and cell lines, we hypothesized that miR-338-3p overexpression might suppress the malignant phenotypes of thyroid cancer cells. The results for *in vitro* cell proliferation, colony formation, migration, invasion, and *in vivo* tumor formation confirmed that ectopic miR-338-3p expression suppressed thyroid cancer cell growth. Altogether, both clinical and experimental data supported a tumor-suppressive role of miR-338-3p in thyroid cancer.

The fundamental function of miRNAs is performed through regulating their target genes

via direct cleavage of mRNA and/or by inhibition of protein synthesis [5]. In this study, we selected AKT3 as a target of miR-338-3p by using bioinformatics-based predictions. AKT3 has been reported to be involved in cancer progression and function as an oncogene in many types of cancers by regulating the PIK3/AKT signal pathway [23-25]. Recently, in a thyroid cancer study, it was found that AKT3 expression was upregulated and that inhibition of AKT3 expression inhibited cell proliferation, migration, and invasion *in vitro* [17]. Notably, AKT3 has been found to be regulated by several miRNAs, such as miR-29a [17] and miR-145 [26]. We identified AKT3 as a target of miR-338-3p in thyroid cancer by using the luciferase reporter assay, qRT-PCR, and western blot. In addition, we found that AKT3 expression was upregulated in thyroid cancer tissues and that its expression level was inversely correlated with miR-338-3p expression in thyroid cancer tissues. Furthermore, AKT3 downregulation and miR-338-3p overexpression had similar inhibitory effects on thyroid cancer cells. The importance of AKT3 in mediating the effect of miR-338-3p was substantiated by the finding that AKT3 overexpression rescued the miR-338-3p-mediated inhibitory effect on thyroid cancer cells.

In conclusion, to our knowledge, our study is the first to provide evidence that miR-338-3p is downregulated in thyroid cancer tissues and cell lines and functions as a tumor suppressor suppressing thyroid cancer growth via targeting AKT3. Identification of the miR-338-3p/AKT3 axis in thyroid cancer would contribute to better understanding of the molecular mechanisms underlying thyroid cancer progression.

Disclosure of conflict of interest

None.

Address correspondence to: Hui Wang, Department of Ultrasound, The China-Japan Union Hospital of Jilin University, Changchun 130033, China. E-mail: wanghui1734@126.com

References

[1] Siegel R, Naishadham D and Jemal A. Cancer statistics, 2013. CA Cancer J Clin 2013; 63: 11-30.

[2] Liu S, Semenciw R, Ugnat AM and Mao Y. Increasing thyroid cancer incidence in Canada, 1970-1996: time trends and age-period-cohort effects. Br J Cancer 2001; 85: 1335-1339.

[3] Pemayun TG. Current diagnosis and management of thyroid nodules. Acta Med Indones 2016; 48: 247-257.

[4] Bushati N and Cohen SM. microRNA functions. Annu Rev Cell Dev Biol 2007; 23: 175-205.

[5] Hwang HW and Mendell JT. MicroRNAs in cell proliferation, cell death, and tumorigenesis. Br J Cancer 2006; 94: 776-780.

[6] Calin GA and Croce CM. MicroRNA signatures in human cancers. Nat Rev Cancer 2006; 6: 857-866.

[7] Tie J, Fan D. Big roles of microRNAs in tumorigenesis and tumor development. Histol Histopathol 2011; 26: 1353-1361.

[8] Aragon Han P, Weng CH, Khawaja HT, Nagarajan N, Schneider EB, Umbricht CB, Witwer KW and Zeiger MA. MicroRNA expression and association with clinicopathologic features in papillary thyroid cancer: a systematic review. Thyroid 2015; 25: 1322-1329.

[9] de la Chapelle A and Jazdzewski K. MicroRNAs in thyroid cancer. J Clin Endocrinol Metab 2011; 96: 3326-3336.

[10] Leonardi GC, Candido S, Carbone M, Colaianni V, Garozzo SF, Cina D and Libra M. microRNAs and thyroid cancer: biological and clinical significance (Review). Int J Mol Med 2012; 30: 991-999.

[11] Zhang P, Shao G, Lin X, Liu Y and Yang Z. MiR-338-3p inhibits the growth and invasion of non-small cell lung cancer cells by targeting IRS2. Am J Cancer Res 2017; 7: 53-63.

[12] Zhang Y, Shi B, Chen J, Hu L and Zhao C. MiR-338-3p targets pyruvate kinase M2 and affects cell proliferation and metabolism of ovarian cancer. Am J Transl Res 2016; 8: 3266-3273.

[13] Chen JS, Liang LL, Xu HX, Chen F, Shen SL, Chen W, Chen LZ, Su Q, Zhang LJ, Bi J, Zeng WT, Li W, Ma N and Huang XH. miR-338-3p inhibits epithelial-mesenchymal transition and metastasis in hepatocellular carcinoma cells. Oncotarget 2016; [Epub ahead of print].

[14] Shang C, Hong Y, Guo Y and Xue YX. Mir-338-3p inhibits malignant biological behaviors of glioma cells by targeting macc1 gene. Med Sci Monit 2016; 22: 710-716.

[15] Chen JT, Yao KH, Hua L, Zhang LP, Wang CY and Zhang JJ. MiR-338-3p inhibits the proliferation and migration of gastric cancer cells by targeting ADAM17. Int J Clin Exp Pathol 2015; 8: 10922-10928.

[16] Guo B, Liu L, Yao J, Ma R, Chang D, Li Z, Song T and Huang C. miR-338-3p suppresses gastric cancer progression through a PTEN-AKT axis by targeting P-REX2a. Mol Cancer Res 2014; 12: 313-321.

[17] Li R, Liu J, Li Q, Chen G and Yu X. miR-29a suppresses growth and metastasis in papillary thyroid carcinoma by targeting AKT3. Tumour Biol 2016; 37: 3987-3996.
[18] Wen Q, Zhao J, Bai L, Wang T, Zhang H and Ma Q. miR-126 inhibits papillary thyroid carcinoma growth by targeting LRP6. Oncol Rep 2015; 34: 2202-2210.
[19] Wang P, Meng X, Huang Y, Lv Z, Liu J, Wang G, Meng W, Xue S, Zhang Q, Zhang P and Chen G. MicroRNA-497 inhibits thyroid cancer tumor growth and invasion by suppressing BDNF. Oncotarget 2017; 8: 2825-2834.
[20] Dong S, Meng X, Xue S, Yan Z, Ren P and Liu J. microRNA-141 inhibits thyroid cancer cell growth and metastasis by targeting insulin receptor substrate 2. Am J Transl Res 2016; 8: 1471-1481.
[21] Xu H, Zhao L, Fang Q, Sun J, Zhang S, Zhan C, Liu S and Zhang Y. MiR-338-3p inhibits hepatocarcinoma cells and sensitizes these cells to sorafenib by targeting hypoxia-induced factor 1alpha. PLoS One 2014; 9: e115565.
[22] Hong-Yuan W and Xiao-Ping C. miR-338-3p suppresses epithelial-mesenchymal transition and metastasis in human nonsmall cell lung cancer. Indian J Cancer 2015; 52 Suppl 3: E168-171.
[23] Bellacosa A, Kumar CC, Di Cristofano A and Testa JR. Activation of AKT kinases in cancer: implications for therapeutic targeting. Adv Cancer Res 2005; 94: 29-86.
[24] Paul-Samojedny M, Pudelko A, Kowalczyk M, Fila-Danilow A, Suchanek-Raif R, Borkowska P and Kowalski J. Combination therapy with akt3 and pi3kca sirna enhances the antitumor effect of temozolomide and carmustine in t98g glioblastoma multiforme cells. BioDrugs 2016; 30: 129-144.
[25] Grottke A, Ewald F, Lange T, Norz D, Herzberger C, Bach J, Grabinski N, Graser L, Hoppner F, Nashan B, Schumacher U and Jucker M. Downregulation of akt3 increases migration and metastasis in triple negative breast cancer cells by upregulating s100a4. PLoS One 2016; 11: e0146370.
[26] Boufraqech M, Zhang L, Jain M, Patel D, Ellis R, Xiong Y, He M, Nilubol N, Merino MJ and Kebebew E. miR-145 suppresses thyroid cancer growth and metastasis and targets AKT3. Endocr Relat Cancer 2014; 21: 517-531.